Large-Scale Spinning Assembly of Neat, Morphology-Defined, Graphene-Based Hollow Fibers

Yang Zhao,[#] Changcheng Jiang,[†,#,∥] Chuangang Hu,[†] Zelin Dong,[†] Jiangli Xue,[†] Yuning Meng,[†] Ning Zheng,[‡] Pengwan Chen,[§] and Liangti Qu[†,*]

[†]Key Laboratory of Cluster Science, Ministry of Education, School of Chemistry, [‡]School of Physics, and [§]State Key Laboratory of Explosion Science and Technology, Beijing Institute of Technology, Beijing 100081, China. [#]Y.Z. and C.J. contributed equally to this work. [∥]Present address: Department of Chemistry and Biochemistry, The Ohio State University, Columbus, Ohio 43210, United States.

ABSTRACT Large-scale assembly of graphenes in a well-controlled macroscopic fashion is important for practical applications. We have developed a facile and straightforward approach for continuous fabrication of neat, morphology-defined, graphene-based hollow fibers (HFs) *via* a coaxial two-capillary spinning strategy. With a high throughput, HFs and necklace-like HFs of graphene oxide have been well-controlled produced with the ease of functionalization and conversion to graphene HFs *via* simply thermal or chemical reduction. This work paves the way toward the mass production of graphene-based HFs with desirable functionalities and morphologies for many of important applications in fluidics, catalysis, purification, separation, and sensing.

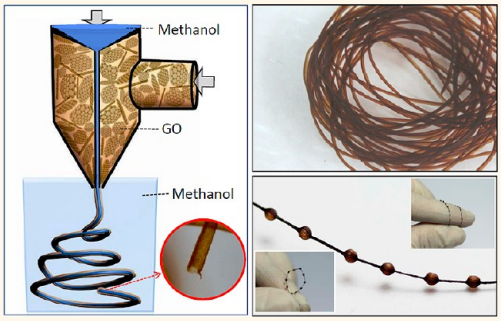

KEYWORDS: graphene · hollow fibers · macroscopic assembly · morphology control · mass production

Graphene, an atom-thick two-dimensional (2D) material comprising monolayer hexagonal sp^2-hybridized carbons, is attracting tremendous attention owing to its fascinating properties such as large electron mobility,[1−3] high thermal conductivity,[4] extraordinary elasticity and stiffness,[5] as well as the relatively low cost for large scale production from natural graphite.[6] The development of scalable assembly methods is the key step toward the practicality of graphenes. For integration of the remarkable properties of individual graphenes into macroscopic, functional structures of practical importance, many efforts have been made to devise an effective assembly strategy for construction of 2D macroscopic configurations[7−12] and 3D frameworks,[13−15] in virtue of the intrinsic 2D structure. However, 1D macroscopic fibers assembled from 2D microcosmic graphene sheets has been recently achieved only by several groups.[16−22] As a new type of carbon-based fiber, graphene fiber possesses the common characteristics of fibers such as mechanical flexibility for textile use, while uniquely possessing low cost, lightweight mass, and ease of functionalization in comparison with conventional carbon fibers.[16−19] In this regard, we have developed a facile dimensionally confined hydrothermal strategy to fabricate macroscopic neat graphene fibers with a strength comparable to carbon nanotube (CNT) yarns from aqueous graphene oxide (GO) suspensions.[18] This fiber is light, shapable, and weavable with ease of *in situ* and postsynthesis functionalization for integration into smart textiles. By developing a dually geometric confinement method, we have also recently achieved the fabrication of multichannel graphene microtubings with a certain length,[23] which stand for newly assembled architectures of graphenes with a hollow interior. These graphene microtubings show promise for stimulus-responsive devices and self-powered micromotors, and are essential for fluidics, catalysis, purification, separation, sensing, and environmental protection.[24−27]

Herein, we report a facile and straightforward approach for continuously engineered production of morphology-controlled graphene-based hollow fibers (HFs) *via*

* Address correspondence to lqu@bit.edu.cn.

Received for review December 8, 2012 and accepted February 14, 2013.

Published online February 14, 2013
10.1021/nn305674a

a coaxial two-capillary spinning strategy. Length-unlimited graphene oxide HFs (GO-HFs) and necklace-like graphene oxide HFs (*n*GO-HFs) with ease of functionalization and conversion to graphene HFs (G-HFs) have been fabricated by direct spinning of a GO suspension. This work paves the way for the mass production of graphene-based HFs with desirable functionalities and morphologies for many important applications.

RESULTS AND DISCUSSION

Figure 1a shows a schematic illustration of our setup for directly spinning of GO-HFs into the coagulation bath of methanol solution containing 3 M KCl. A coaxial two-capillary spinneret was exploited to conveniently fabricate the GO-HFs. The spinneret was fabricated by inserting a stainless steel needle (with an inner diameter of *ca.* 300 μm and outer diameter of *ca.* 500 μm) into a branched glass tube with a capillary tip (inner diameter of *ca.* 1000 μm). The coaxial two-capillary spinneret is shown in Figure 1b. Besides the spinneret used to define the tubular shape, a high concentration of GO suspension is required for formation of GO-HFs. Figure 1c shows the GO solution of 20 mg/mL with a viscosity of 2.3 $\times$ 10^3 Pa·s, which was prepared by gradually evaporating the water of dilute GO solution. The GO has a size distribution of 0.5 to 4 μm (Supporting Information, Figure S1) and its suspension is viscous enough to ensure the effective coagulation during continuously spinning into the bath of KCl/methanol solution.[16,17,28] In a typical experiment (Figure 1d), the stainless steel needle is connected to a syringe-containing coagulation bath, while the glass tube is filled with GO suspension through the branch. An air pressure is applied to the branch to push the GO out of the spinneret and into the bath solution, accompanied with a flow of the coagulation solution at a proper rate out from the core capillary that is controlled by the injection pump, and the GO-HFs are continuously produced (Supporting Information, movie S1).

The continuous production of GO-HFs is very fast and efficient. One meter of GO-HFs is generated within 30 s with a production rate of 3.3 cm/s. In fact, the throughput can be further enhanced by accelerating the flow of GO suspension. Figure 1e presents a roll of initially produced GO-HFs collected in KCl/methanol solution. The close view of the fibers reveals the semitransparent character (Figure 1f) and the hollow structure is reflected by the open tip (Figure 1f, inset). After being fully washed with clean methanol and naturally dried at room temperature, the flexible and mechanically stable GO-HFs shrink a little in diameter without any structural collapse and are readily rolled in discoid shape for further use (Figure 1g and Supporting Information, Figure S2). The X-ray diffraction (XRD) pattern exhibited the typical feature of GO with a $2\theta = 11°$ (Supporting Information, Figure S3). The directly spun

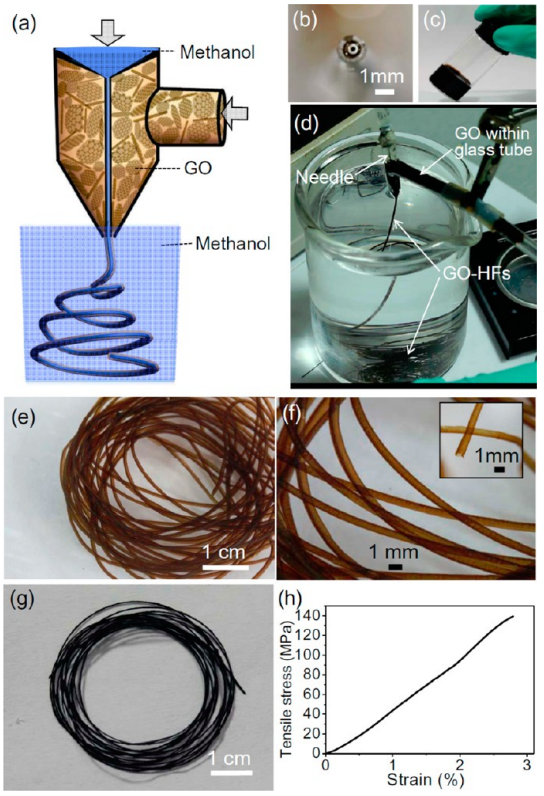

Figure 1. (a) Schematic illustration of the setup that used a dual-capillary spinneret to directly spin GO-HFs. (b) A photo of the coaxial two-capillary spinneret. (c) The concentrated GO suspension (20 mg/mL) for spinning. (d) The experimental setup for directly spinning GO-HFs. (e,f) Photos of the spun GO-HFs in methanol solution with 3 M KCl. The inset in panel f shows the open tip of one GO-HF. (g) A photo of the naturally dried GO-HFs. (h) Typical stress–strain curve of a single GO-HF.

GO-HFs have a measured tensile strength of up to *ca.* 140 MPa (Figure 1h), which is even comparable to that of solid GO fiber[16,17] and filtration-formed GO papers.[7,29] The GO-HFs have a typical elongation at break of about 2.8% presumably originating from the possible displacement of the GO sheets within the walls,[18] which is much larger than that of graphite fibers (about 1%).

The initially produced GO-HFs has an incompact but highly cross-linking structure of random graphene sheets interlaced within the wall (Figure 2a) similar to that 3D graphene framework,[30,31] while it seems that GO sheets on the inner and outer surfaces lie along the tube axis (Figure 2b,c and Supporting Information, Figure S4) probably induced by the extrusion process, which may be beneficial to the high strength. After drying, the pore-rich structures become densely stacked both on the surface and within the wall (Figure 2d–f). Compact stacks of GO sheets (Figure 2d) supersede the foam structure within the wall (Figure 2a), and a seamless surface (Figure 2e,f), in spite of wrinkles there, replaces the porous one (Figure 2b,c). As a result, the diameter of *ca.* 700 μm for the GO-HF at the "wet" stage (Figure 2a,b) reduces to *ca.* 470 μm for the dry one with a continuously

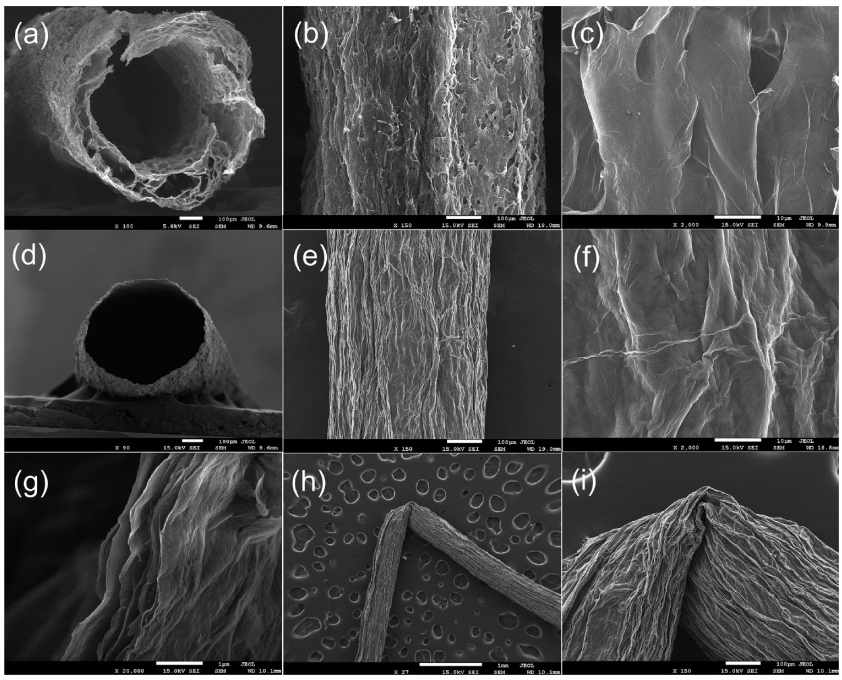

Figure 2. (a−c) Scanning electron microscope (SEM) images of the cross-section and surface of initially produced GO-HF with rapidly freeze-dried treatment. (d−f) SEM images of naturally dried GO-HF samples. (g) Cross-section view of the wall of GO-HF. (h,i) SEM images of a folded GO-HF. Scale bars: (a,b,d,e,i) 100 μm; (c,f) 10 μm; (g) 1 μm; (h) 1 mm.

hollow structure (Supporting Information, Figure S5). Since there is tight layer-by-layer stacking of GO sheets (~1 μm in thickness) within the wall (Figure 2g), the GO-HFs have a considerable tolerance to the bending and folding. As it is being bent, the GO-HF deforms the wall accordingly in the absence of any broken points (Figure 2h,i). Further, both the thickness of wall and the inner/outer diameter of GO-HFs can be tuned accordingly by the proper spinneret design and the change of GO concentration as exemplified in Supporting Information, Figures S6−S9.

The direct-spin strategy developed in this study also allows the simultaneous functionalization of GO-HFs. The modification of GO-HFs can be done readily by simply introducing the functional components into the core flow or mixing the targets with the initial GO suspension during GO-HF production, respectively. As exemplified in Figure 3a−c, when the SiO_2 nanospheres (*ca.* 200 nm) as model component are mingled within the flow medium of KCl/methanol in the inner capillary of the spinneret, nanospheres that are region confined are attached to the inner-wall surface of the GO-HF, while the outer-wall surface reamins intact. On the other hand, the premixing of fluorescent components into the GO suspension will produce the luminescent GO-HF despite the possible fluorescence quenching (Figure 3d,e and Supporting Information, Figure S10). The physical incorporation of functional components into GO-HFs (Supporting Information, Figure S11) demonstrates the feasibility of simultaneous functionalization of GO-HFs during production.

The as-produced GO-HFs can be conveniently converted to G-HFs by thermal annealing at a certain temperature (*e.g.*, 400 °C) without loss of their flexibility but with enhanced mechanical strength (Supporting Information, Figure S12). Similarly, G-HFs can also be obtained by chemical reduction using hydroiodic acid as the reducing agent[32] and have a negligible morphologic change with a uniform hollow structure (Supporting Information, Figures S13 and S14). The generated G-HFs have an electric conductivity of 8−10 S/cm measured by a four probe method, which is close to that of graphene fibers.[16,18] G-HFs with fast photocurrent response and good repeatability have also been demonstrated by immobilizing TiO_2 particles within the G-HF walls (Supporting Information, Figure S15).

The concentrated GO suspension with high viscosity allows it to be directly bubbled (Supporting Information, Figure S16), thus providing the chance to elaborately tune the morphologic character of the resultant GO-HFs. We have replaced the inner fluid of KCl/methanol solution with compressed air (Supporting Information, Figure S17). The obtained GO-HF displays a necklace-like structure where each of the microspheres is connected by the fiber (Figure 4a). Like the flexibility of the aforementioned GO-HF, the *n*GO-HF can be pliably rolled around a finger (Figure 4b) and bent to a circle shape intact (Figure 4b, inset). These microspheres have a diameter of *ca.* 700 μm (Figure 4c), and their surfaces are composed of compact GO films (Figure 4d) similar to that of GO-HFs (Figure 2f). The deliberately opened microbead in Figure 4e clearly presents the hollow interior, and a

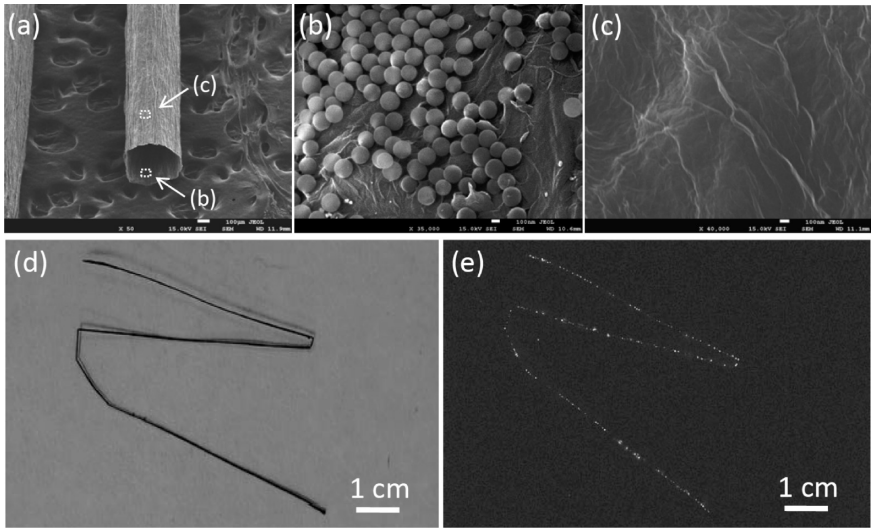

Figure 3. (a) SEM image of a GO-HF inner-wall modified with SiO_2 nanospheres. (b,c) SEM images corresponding to inner and outer surfaces of GO-HF as marked in panel a, respectively. (d,e) Photos of the fluorescent nanoparticles-intercalated GO-HF without and with irradiation of 365 nm UV lamp, respectively. Scale bars: (a) 100 μm; (b,c) 100 nm.

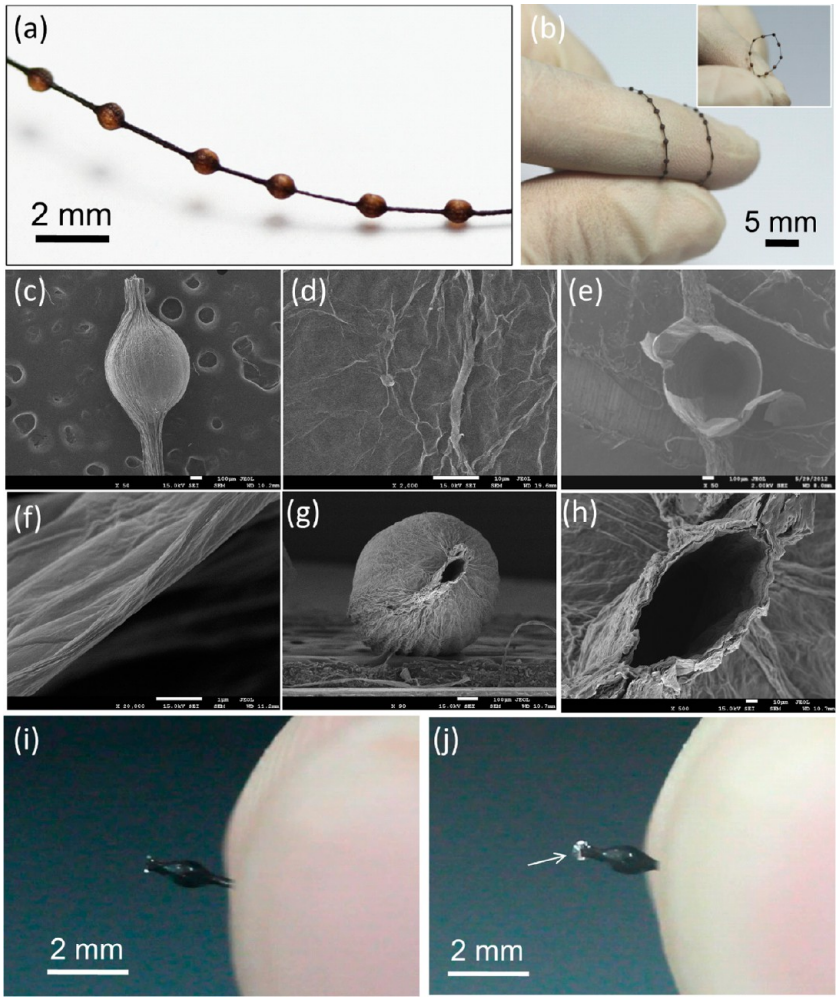

Figure 4. (a) A photo of *n*GO-HF generated with the air flow rate of 1.0 mL/min. (b) A photograph of the *n*GO-HF coiled around a finger and bent to the circle shape (inset). (c) A single microsphere of the *n*GO-HF and (d) the corresponding enlarged surface image. (e,f) SEM images of a broken microsphere and its edge, respectively. (g,h) The cross-section view of the *n*GO-HF broken between microspheres. (i) A photo of a short *n*GO-HF sucked with soap-suds on one side, and (j) a soap bubble is generated on its tip by pressing the bubble of *n*GO-HF. Scale bars: (c,e,g) 100 μm; (f) 1 μm; (d,h) 10 μm.

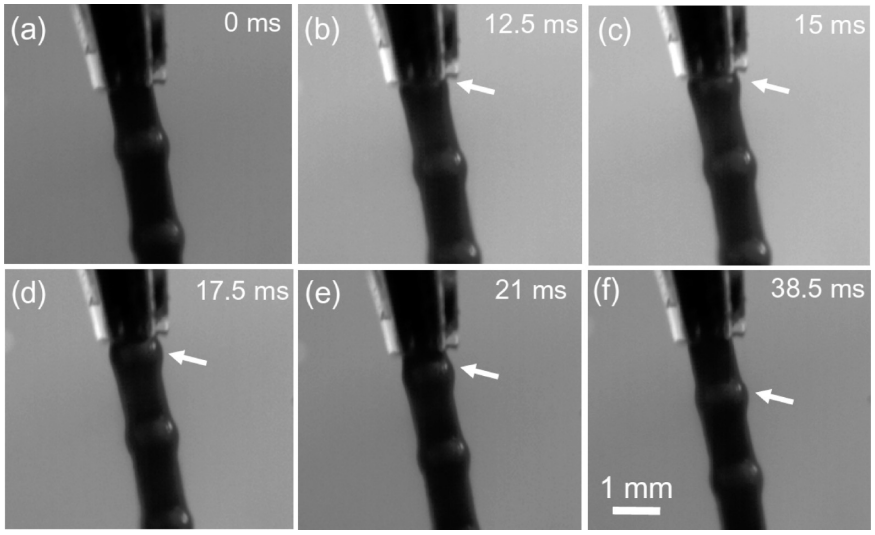

Figure 5. The snapshot of the bubble formation along *n*GO-HF during spinning at the air flow rate of 1.5 mL/min.

high magnification view of its wall exhibits densely stacked GO layers with a thickness of only *ca*. 200 nm (Figure 4f). Figure 4 panels g and h show the hollow microsphere has a channel with a diameter of *ca*. 100 μm connected with the outside fiber, indicating the hollow channel is running through the whole *n*GO-HF (Supporting Information, Figure S18). Despite the necklace-like structure, the tensile strength of *n*GO-HF was measured to be as high as *ca*. 150 MPa on the basis of the fiber diameter of *ca*. 100 μm. The *n*GO-HF also has a relatively large elongation of about 6% at break due to the elastic deformation of the hollow microspheres within *n*GO-HF (Supporting Information, Figure S19). The hollow microspheres along *n*GO-HF can tolerate the compression to a large extent. As demonstrated in Figure 4i, a short *n*GO-HF was precoated with polydimethylsiloxane (PDMS) and sealed in one end. Once sucked with soap-suds and pressed by fingers on the hollow microsphere of *n*GO-HF, a soap bubble can be generated on its tip with high repeatability (Figure 4j), which presents the great potential of *n*GO-HF for use as a micropump system.

The *n*GO-HFs have a relatively smaller fiber diameter excluding the microspheres than that of the aforementioned GO-HFs (Figure 2), which is probably because the absence of coagulation solution within the hollow GO fibers could lead to their shrinkage toward the void of spun samples, and is also possibly induced by the effect of air pressure on the GO walls during spinning. Despite the difficulty in determining the congregated air pressure within the GO-HFs during spinning and the detailed formation mechanism of *n*GO-HFs in the preliminary study, we indeed can exquisitely regulate the distribution of these microspheres along the fiber by control over the air flow rate. With the increase of air flow rate from 1.0 mL/min to 2.0 mL/min, the density of microspheres along the fiber gradually increases (Supporting Information, Figures S20 and S21). Supporting Information, movie S2 displays the continuous production of *n*GO-HFs at an air flow rate of 1.5 mL/min and a GO injection velocity of 0.1 mL/s. At a relatively high air flow rate of 2.0 mL/min, the as-prepared *n*GO-HFs show a close bubble-by-bubble connection (Supporting Information, Figure S20c and S22). Accordingly, these *n*GO-HFs can also be converted into *n*G-HFs by thermal annealing or chemical reduction using hydroiodic acid as reducing agent (Supporting Information, Figure S23).

We have followed up the formation of bubbles along GO-HFs within a KCl/methanol bath during the spinning process. As revealed in Figure 5 and Supporting Information, Movie S3, accompanying with the extrusion of GO-HF with a diameter defined by spinneret, an intumescent bubble gradually forms due to the congregated pressure of air flow (Figure 5a–d). Its shape is solidified rapidly within 10 ms and remains unchanged in the KCl/methanol bath despite the constant flow of air through the core (Figure 5d–f). The continuous extrusion of GO-HF with alternate formation of bubbles produces the final *n*GO-HFs. The wet *n*GO-HFs produced initially have a relatively large diameter, which shrinks to the final necklace-like structure after drying (Supporting Information, Figure S24).

CONCLUSIONS

We have demonstrated a direct spinning strategy for continuously engineered production of neat, morphology-defined, graphene-based hollow microfibers on a large scale with a high throughput. Both GO-HFs and *n*GO-HFs have been well-controlled produced with ease of functionalization and conversion to G-HFs and *n*G-HFs *via* thermal or chemical reduction. This work paves the way toward the mass production of graphene-based HFs with desirable functionalities and morphologies. Beyond the examples presented in the

preliminary study, the well-defined functional GO-HFs and *n*GO-HFs system will also play essential roles in other important fields such as fluidics, catalysis, purification, separation, and sensing.

EXPERIMENTAL SECTION

Preparation of Graphene Oxide Hollow Fibers (GO-HFs). GO was prepared by using the modified Hummer method as reported in our previous papers.[6,23,31] The coaxial two-capillary spinneret was homemade and used for producing the GO-HFs. In this study, the inner capillary is a stainless steel needle that is connected to a 10 mL syringe containing methanol solution with 3 M KCl, while the outer glass capillary is filled with a GO suspension (20 mg/mL) through the branch. The KCl/methanol flow rate within the core capillary is set at 0.6 mL/min and the injection velocity of the GO suspension is 0.1 mL/s. The GO-HFs were reduced to G-HFs by using hydroiodic acid as the reduction agent at 80 °C for 8 h or by using thermal annealing at 400 °C in the air for 1 h.

Preparation of GO-HFs Inner Surface Modified with SiO_2. The mixture of SiO_2 (*ca.* 200 nm) and KCl/methanol solution was produced by mixing 0.5 mL of SiO_2 suspension (5% (w/v)) with 3 M KCl/methanol solution (15 mL), which was injected into the inner capillary for formation of GO-HFs.

Preparation of Fluorescent GO-HFs. Fluorescent powder with a particle size of *ca.* 30−50 μm was received from Beijing chemical factory. A 10 mg portion of fluorescent powder was mixed with 10 mL of GO suspension (20 mg/mL) for the direct spinning of GO-HFs as mentioned above.

Preparation of Necklace-like Graphene Oxide HFs (*n*GO-HFs). For formation of *n*GO-HFs, the inner capillary of the spinneret was pumped with air instead of the KCl/methanol solution. At a set flow rate of 1, 1.5, and 2 mL/min, *n*GO-HFs are continuously produced. *n*G-HFs were obtained by thermal or chemical reduction of *n*GO-HFs as mentioned above.

Characterization. The morphology of prepared samples was carried out by scanning electron microscope (SEM, JSM-7500F). X-ray diffraction (XRD) patterns were obtained by using a PW-1710 (Philips, Netherlands) diffractometer with graphite monochromatized Cu Kα irradiation (λ = 1.54 Å). Fourier transform infrared (FT-IR) spectra were recorded on a Bruker spectrometer (Equinox 55/S) using KBr pellets. Mechanical tests were carried out by SHIMADZU AGS-X with a strain rate of 1 mm/min. All data were collected as the failure happened at the middle region of the testing samples. The viscosity of GO suspensions was tested by a NDJ-1 rotational viscometer (Yueping Scientific Instrument, Shanghai). The movies and photos of the *n*GO-HF formation are taken by the high speed camera (Phantom v7.3).

Conflict of Interest: The authors declare no competing financial interest.

Supporting Information Available: Additional figures and movies as described in the text. This material is available free of charge *via* the Internet at http://pubs.acs.org.

Acknowledgment. We thank the financial support from National Basic Research Program of China (2011CB013000) and NSFC (21174019, 51161120361).

REFERENCES AND NOTES

1. Novoselov, K. S.; Geim, A. K.; Morozov, S. V.; Jiang, D.; Zhang, Y.; Dubonos, S. V.; Grigorieva, I. V.; Firsov, A. A. Electric Field Effect in Atomically Thin Carbon Films. *Science* **2004**, *306*, 666–669.
2. Novoselov, K. S.; Geim, A. K.; Morozov, S. V.; Jiang, D.; Katsnelson, M. I.; Grigorieva, I. V.; Dubonos, S. V.; Firsov, A. A. Two-Dimensional Gas of Massless Dirac Fermions in Graphene. *Nature* **2005**, *438*, 197–200.
3. Zhang, Y.; Tan, Y. W.; Stormer, H. L.; Kim, P. Experimental Observation of the Quantum Hall Effect and Berry's Phase in Graphene. *Nature* **2005**, *438*, 201–204.
4. Balandin, A. A.; Ghosh, S.; Bao, W.; Calizo, I.; Teweldebrhan, D.; Miao, F.; Lau, C. N. Superior Thermal Conductivity of Single-Layer Graphene. *Nano Lett.* **2008**, *8*, 902–907.
5. Lee, C.; Wei, X. D.; Kysar, J. W.; Hone, J. Measurement of the Elastic Properties and Intrinsic Strength of Monolayer Graphene. *Science* **2008**, *321*, 385–388.
6. Li, Y.; Zhao, Y.; Cheng, H.; Hu, Y.; Shi, G. Q.; Dai, L. M.; Qu, L. T. Nitrogen-Doped Graphene Quantum Dots with Oxygen-Rich Functional Groups. *J. Am. Chem. Soc.* **2012**, *134*, 15–18.
7. Dikin, D. A.; Stankovich, S.; Zimney, E. J.; Piner, R. D.; Dommett, G. H. B.; Evmenenko, G.; Nguyen, S. T.; Ruoff, R. S. Preparation and Characterization of Graphene Oxide Paper. *Nature* **2007**, *448*, 457–460.
8. Chen, H.; Müller, M. B.; Gilmore, K. J.; Wallace, G. G.; Li, D. Mechanically Strong, Electrically Conductive, and Biocompatible Graphene Paper. *Adv. Mater.* **2008**, *20*, 3557–3561.
9. Li, D.; Müller, M. B.; Gilje, S.; Kaner, R. B.; Wallace, G. G. Processable Aqueous Dispersions of Graphene Nanosheets. *Nat. Nanotechnol.* **2008**, *3*, 101–105.
10. Li, X.; Sun, P. Z.; Fan, L. L.; Zhu, M.; Wang, K. L.; Zhong, M. L.; Wei, J. Q.; Wu, D. H.; Cheng, Y.; Zhu, H. W. Multifunctional Graphene Woven Fabrics. *Sci. Rep.* **2012**, *2*, 395.
11. Eda, G.; Fanchini, G.; Chhowalla, M. Large-Area Ultrathin Films of Reduced Graphene Oxide as a Transparent and Flexible Electronic Material. *Nat. Nanotechnol.* **2008**, *3*, 270–274.
12. Li, X. L.; Zhang, G.; Bai, X.; Sun, X.; Wang, X.; Wang, E.; Dai, H. Highly Conducting Graphene Sheets and Langmuir−Blodgett Films. *Nat. Nanotechnol.* **2008**, *3*, 538–542.
13. Chen, Z. P.; Ren, W. C.; Gao, L. B.; Liu, B. L.; Pei, S. F.; Cheng, H. M. Three-Dimensional Flexible and Conductive Interconnected Graphene Networks Grown by Chemical Vapour Deposition. *Nat. Mater.* **2011**, *10*, 424–428.
14. Xu, Y.; Sheng, K.; Li, C.; Shi, G. Self-Assembled Graphene Hydrogel *via* a One-Step Hydrothermal Process. *ACS Nano* **2010**, *4*, 4324–4330.
15. Lee, S. H.; Kim, H. W.; Hwang, O.; Lee, W. J.; Kwon, J.; Bielawski, C. W.; Ruoff, R. S.; Kim, S. O. Three-Dimensional Self-Assembly of Graphene Oxide Platelets into Mechanically Flexible Macroporous Carbon Films. *Angew. Chem., Int. Ed.* **2010**, *49*, 10084–10088.
16. Xu, Z.; Gao, C. Graphene Chiral Liquid Crystals and Macroscopic Assembled Fibres. *Nat. Commun.* **2011**, *2*, 57110.1038/ncomms1583.
17. Xu, Z.; Sun, H. Y.; Zhao, X. L.; Gao, C. Ultrastrong Fibers Assembled from Giant Graphene Oxide Sheets. *Adv. Mater.* **2013**, *25*, 188–19310.1002/adma.201203448.
18. Dong, Z. L.; Jiang, C. C.; Cheng, H. H.; Zhao, Y.; Shi, G. Q.; Jiang, L.; Qu, L. T. Facile Fabrication of Light, Flexible and Multifunctional Graphene Fibers. *Adv. Mater.* **2012**, *24*, 1856–1861.
19. Cong, H. P.; Ren, X. C.; Wang, P.; Yu, S. H. Wet-Spinning Assembly of Continuous, Neat, and Macroscopic Graphene Fibers. *Sci. Rep.* **2012**, 10.1038/srep00613.
20. Carretero−González, J.; Castillo−Martínez, E.; Dias−Lima, M.; Acik, M.; Rogers, D. M.; Sovich, J.; Haines, C. S.; Lepró, X.; Kozlov, M.; Zhakidov, A.; *et al.* Oriented Graphene Nanoribbon Yarn and Sheet from Aligned Multiwalled Carbon Nanotube Sheets. *Adv. Mater.* **2012**, *24*, 5695–5701.
21. Hu, X. Z.; Xu, Z.; Gao, C. Multifunctional, Supramolecular, Continuous Artificial Nacre Fibres. *Sci. Rep.* **2012**, *2*, 767.
22. Xu, Z.; Zhang, Yuan.; Li, P. G.; Gao, C. Strong, Conductive, Lightweight, Neat Graphene Aerogel Fibers with Aligned Pores. *ACS Nano* **2012**, *6*, 7103–7113.
23. Hu, C. G.; Zhao, Y.; Cheng, H. H.; Wang, Y. H.; Dong, Z. L.; Jiang, C. C.; Zhai, X. Q.; Jiang, L.; Qu, L. T. Graphene Microtubings: Controlled Fabrication and Site-Specific Functionalization. *Nano Lett.* **2012**, *12*, 5879–5884.
24. Zhao, Y.; Cao, X.; Jiang, L. Bio-Mimic Multichannel Microtubes by a Facile Method. *J. Am. Chem. Soc.* **2007**, *129*, 764–765.

25. Li, D.; McCann, J.; Xia, Y. Use of Electrospinning to Directly Fabricate Hollow Nanofibers with Functionalized Inner and Outer Surfaces. *Small* **2005**, *1*, 83–86.
26. Baughman, R.; Zakhidov, A.; de Heer, W. Carbon Nanotubes the Route Toward Applications. *Science* **2002**, *297*, 787–792.
27. Martin, C. Nanomaterials—A Membrane-Based Synthetic Approach. *Science* **1994**, *266*, 1961–1966.
28. Steinmetz, J.; Glerup, M.; Paillet, M.; Bernier, P.; Holzinger, M. Production of Pure Nanotube Fibers Using a Modified Wet-Spinning Method. *Carbon* **2005**, *43*, 2397–2429.
29. Compton, O. C.; Nguyen, S. T. Graphene Oxide, Highly Reduced Graphene Oxide, and Graphene: Versatile Building Blocks for Carbon-Based Materials. *Small* **2010**, *6*, 711–723.
30. Hu, C. G.; Cheng, H. H.; Zhao, Y.; Hu, Y.; Liu, Y.; Dai, L. M.; Qu, L. T. Newly-Designed Complex Ternary Pt/PdCu Nanoboxes Anchored on Three-Dimensional Graphene Framework for Highly Efficient Ethanol Oxidation. *Adv. Mater.* **2012**, *24*, 5493–5498.
31. Zhao, Y.; Hu, C. G.; Hu, Y.; Cheng, H. H.; Shi, G. Q.; Qu, L. T. A Versatile, Ultralight, Nitrogen-Doped Graphene Framework. *Angew. Chem., Int. Ed.* **2012**, *51*, 11371–11375.
32. Pei, S.; Zhao, J.; Du, J.; Ren, W.; Cheng, H. M. Direct Reduction of Graphene Oxide Films into Highly Conductive and Flexible Graphene Films by Hydrohalic Acids. *Carbon* **2010**, *48*, 4466–4474.